A novel scheme for solving the oblique derivative boundary-value problem

MAREK MACÁK, ZUZANA MINARECHOVÁ* AND KAROL MIKULA

Department of Mathematics and Descriptive Geometry, Faculty of Civil Engineering, Slovak University of Technology, Radlinského 11, 813 68 Bratislava, Slovakia (macak@math.sk, minarechova@math.sk, mikula@math.sk)

* Corresponding author

Received: June 26, 2013; Revised: October 30, 2013; Accepted: March 17, 2014

ABSTRACT

The paper is devoted to a novel scheme for solving the boundary-value problem (BVP) with the oblique derivative boundary condition (BC). In this approach, the oblique derivative in the BC is decomposed into its normal and two tangential components which are approximated by means of numerical solution values. Then the numerical scheme by the finite volume method is developed and testing numerical experiments are done. The obtained numerical solutions are compared to the exact one to show that the proposed method is second order accurate. Afterwards, the algorithm is applied to solving the fixed gravimetric BVP, namely, the numerical solution is sought in a domain bounded by a part of the Earth's surface (Himalaya region or Slovakia), four side boundaries and a corresponding upper boundary at the satellite level. On the Earth's surface, the oblique derivative BC in the form of surface gravity disturbances from the EGM2008, DTU10-GRAV or the detailed gravity mapping is taken into account. On the upper and side boundaries, the Dirichlet BC from the EGM2008 or GOCO03s is applied. The disturbing potential as a direct numerical result is compared with the solution to the more common BVP with the Neumann BC considered on the Earth's surface. All numerical experiments show better agreement of the solution to the BVP with the oblique derivative BC than solution to the BVP with the Neumann BC in comparison with the disturbing potential obtained by a different mathematical approach. In area of Slovakia, when applying the GPS/levelling test at 61 points, we have gained 1.7 cm improvement in favour of the standard deviation of residuals of quasigeoidal heights obtained by solving the BVP with the oblique derivative BC in comparison with the solution to BVP with the Neumann BC.

Keywords: fixed gravimetric boundary-value problem, oblique derivative boundary condition, finite volume method

1. INTRODUCTION

The main goals of physical geodesy are the precise determination of the external gravity field and the geoid which can be both achieved by solving the external geodetic boundary-value problem (BVP). From the mathematical point of view, the linearized

Stud. Geophys. Geod., 58 (2014), 556–570, DOI: 10.1007/s11200-013-0340-x

geodetic BVP is formulated in the form of the Laplace partial differential equation for the unknown disturbing potential in the external domain. Various boundary conditions (BCs) defined on the Earth's surface can be considered, e.g. classically the Newton BC is prescribed, if the so-called gravity anomalies are used, or the Neumann BC is applied, if the so-called gravity disturbances are used. Recently, also a Dirichlet BC has been considered in case of geodetic BVP solved in bounded domains. In such approaches, the Neumann or Newton BCs are given on the Earth's surface and the Dirichlet BC on the other boundaries, e.g. on the sphere far from the Earth's surface, is applied (see e.g. *Fašková et al., 2010*).

In this paper, we consider (i) the normal derivative of the unknown potential to be given on the part of Earth's surface, i.e. the Neumann BC (the same approach has been used e.g. in *Fašková et al., 2010*), and (ii) the oblique derivative of the unknown potential applied on the Earth's surface, i.e. the oblique derivative BC. On the other parts of the boundary, namely four side walls and a top, the Dirichlet BC is considered.

Several researchers have applied some of numerical methods to the solution of the geodetic BVPs. The boundary element method solving the boundary integral form of the geodetic BVPs has been investigated in e.g. *Klees (1995)*, *Klees et al. (2001)*, *Čunderlík et al. (2008)*. Variational method based on a weak form of the geodetic BVP and a minimization of the quadratic functional has been used in e.g. *Holota (1997)*, *Holota and Nesvadba (2008)*. The finite element method for solving the geodetic BVP with the Neumann and the Dirichlet BC has been studied e.g. in *Fašková et al. (2010)*. In our approach we will apply another numerical method - the finite volume method (FVM).

The paper is organized as follows. In Section 2, we formulate the BVP with the oblique derivative BC. In Section 3, we derive its solution by the FVM where we pay attention to details of incorporating of the oblique derivative BC into the numerical scheme. Section 4 is devoted to the numerical experiments. We start by theoretical numerical experiments with an artificial oblique vector created at first by shifting the center point and later by an adding a rotation. We study the experimental order of convergence of the proposed numerical scheme. Then we focus on practical numerical experiments. In the experiment in the Himalaya region, we solve both, the BVP with the oblique derivative BC and the BVP with the Neumann BC, using EGM2008 (*Pavlis et al., 2008*) data as BC. We compare both solutions with the disturbing potential generated from EGM2008 directly. Then we use the same computational domain as before only the input surface gravity disturbances are generated from the DTU10-GRAV (*Andersen, 2010*) and the disturbing potential from GOCO03S (*Mayer-Gürr et al., unpublished data*). Finally, we present experiment in the area of Slovakia with the input surface gravity disturbances obtained from the detailed gravity mapping and the GPS/leveling test is used to evaluate numerical solutions.

2. FORMULATION OF THE OBLIQUE DERIVATIVE BOUNDARY-VALUE PROBLEM

Let us consider the fixed gravimetric BVP, cf. *Koch and Pope (1972)*, *Bjerhammar and Svensson (1983)*, *Holota (1997)*:

$$\Delta T(\boldsymbol{x}) = 0, \quad \boldsymbol{x} \in R^3 - S, \tag{1}$$

$$\left\langle \nabla T(\boldsymbol{x}), \boldsymbol{s}(\boldsymbol{x}) \right\rangle = -\delta g(\boldsymbol{x}), \quad x \in \partial S, \tag{2}$$

$$T(\boldsymbol{x}) \to 0 \quad \text{as} \quad |\boldsymbol{x}| \to \infty, \tag{3}$$

where S is the Earth body, $T(\boldsymbol{x})$ is the disturbing potential defined as the difference between the real $W(\boldsymbol{x})$ and the normal $U(\boldsymbol{x})$ gravity potential at any point $\boldsymbol{x}$, $\delta g(\boldsymbol{x})$ is the so-called gravity disturbance and $\boldsymbol{s}(\boldsymbol{x}) = -\nabla U(\boldsymbol{x}) / |\nabla U(\boldsymbol{x})|$ is the unit vector normal to the equipotential surface of the normal potential U at point $\boldsymbol{x}$.

Despite the fact that the fixed gravimetric BVP (Eqs (1)–(3)) deals with the infinite domain, in our FVM approach we have constructed a bounded domain Ω in the external space above the Earth, see Fig. 1. The bottom surface $\Gamma \subset \partial\Omega$ represents a part of the Earth's surface ∂S. It is given by a sphere or ellipsoid with the oblique derivative BC prescribed for it. On the upper spherical boundary as well as on the side ones, the Dirichlet BC is considered.

We consider the following BVP in the bounded domain Ω described in the above paragraph:

$$\Delta T(\boldsymbol{x}) = 0, \quad \boldsymbol{x} \in \Omega, \tag{4}$$

$$\left\langle \nabla T(\boldsymbol{x}), \boldsymbol{s}(\boldsymbol{x}) \right\rangle = -\delta g(\boldsymbol{x}), \quad x \in \Gamma, \tag{5}$$

$$T(\boldsymbol{x}) = T_{\mathrm{SAT}}(\boldsymbol{x}), \quad \boldsymbol{x} \in \partial\Omega - \Gamma, \tag{6}$$

where T_{SAT} represents the disturbing potential generated from chosen satellite geopotential model.

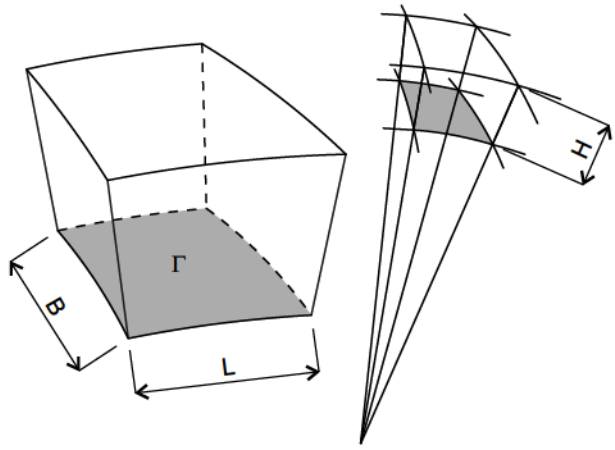

Fig. 1. Sketch of the computational domain Ω. The shaded boundary Γ represents the part of the Earth's surface. *H*: height, *B*: latitude, *L*: longitude.

Solution to the BVP given by Eqs (4)–(6) will be compared with the solution to the BVP with the Neumann BC (see e.g. *Fašková et al., 2010*), where the Neumann BC instead of the oblique derivative BC is considered. To get the Neumann BC, the oblique derivative BC in Eq. (5) is projected onto the normal n_Γ to the boundary Γ

$$\frac{\partial T(\boldsymbol{x})}{\partial n_\Gamma} \approx -\delta g(\boldsymbol{x}) \cos \mu(\boldsymbol{x}), \tag{7}$$

where $\mu(\boldsymbol{x})$ is the angle $\measuredangle(\boldsymbol{s}(\boldsymbol{x}), \boldsymbol{n}_\Gamma(\boldsymbol{x}))$. The same idea was also published in *Čunderlík et al. (2008)*.

3. SOLUTION TO THE OBLIQUE DERIVATIVE BOUNDARY-VALUE PROBLEM BY THE FINITE VOLUME METHOD

The FVM offers an intuitive and conservative way of discretizing the governing equation in a manner that combines some advantages of the finite difference method with some advantages of the finite element method. The general discretization approach is to divide the computational domain Ω into finite volumes p and integrate the equation over each finite volume with the divergence theorem that turns the volume integrals into surface integrals. Then the resulting discretized equations equate fluxes across finite volumes to sources and sinks inside the volume, so the finite volume formulation is conservative because the ux owing across a shared volume face is the same for each adjoining volume.

So in the aforementioned manner we multiply the Laplace equation (4) by –1 and then by integrating

$$-\int_p \Delta T \, dx \, dy \, dz = -\int_{\partial p} \nabla T \cdot \boldsymbol{n} \, d\sigma \tag{8}$$

we obtain for every finite volume p

$$-\int_{\partial p} \frac{\partial T}{\partial n} \, d\sigma = 0. \tag{9}$$

Let $q \in N_p$ be a neighbour of the finite volume p, where N_p denotes all neighbours of p. Then T_p and T_q are approximate values of T in p and q, e_{pq} is a boundary of the finite volume p that is common with q. Vector $\boldsymbol{n}_{pq}$ is a unit normal vector oriented from p to q and it is orthogonal to e_{pq}. By $m(e_{pq})$ we denote the area of e_{pq}. Let x_p and x_q be representative points of p and q (e.g. centers of gravity) and d_{pq} distance between them. If we approximate the normal derivative along the boundary of the finite volume p by

$$\frac{\partial T}{\partial n_{pq}} \approx \frac{\sim T_q - T_p}{d_{pq}}, \tag{10}$$

we obtain from Eqs (9) and (10)

$$-\sum_{q \in N_p} \frac{T_q - T_p}{d_{pq}} m\left(e_{pq}\right) = 0, \tag{11}$$

which can be written in the form

$$\sum_{q \in N_p} \frac{m\left(e_{pq}\right)}{d_{pq}} \left(T_p - T_q\right) = 0, \tag{12}$$

representing the linear system of algebraic equations for the FVM. The term $m\left(e_{pq}\right)/d_{pq}$ defined on sides of the finite volume p is the so-called transmissivity coefficient, see *Eymard (2001)*. To take BCs into account, in case of the Dirichlet BC (Eq. (6)) we prescribe the value of T_q on the boundary, while in case of the oblique derivative BC (Eq. (5)), a special treatment is needed that will be discussed in the following subsection.

3.1. The oblique derivative boundary condition

In this section we deal with the numerical solution to the oblique derivative BVP Eqs (4)–(6). We start by splitting the gradient in Eq. (5) into one normal and two tangential directions

$$\nabla T = \left\langle \nabla T, \boldsymbol{n} \right\rangle \boldsymbol{n} + \left\langle \nabla T, \boldsymbol{t}_1 \right\rangle \boldsymbol{t}_1 + \left\langle \nabla T, \boldsymbol{t}_2 \right\rangle \boldsymbol{t}_2 = \frac{\partial T}{\partial n}\boldsymbol{n} + \frac{\partial T}{\partial t_1}\boldsymbol{t}_1 + \frac{\partial T}{\partial t_2}\boldsymbol{t}_2, \tag{13}$$

where $\boldsymbol{n}$ is the normal vector and $\boldsymbol{t}_1$, $\boldsymbol{t}_2$ are linearly independent tangent vectors to $\Gamma \subset \partial\Omega \subset R^3$. Then by inserting Eq. (13) to Eq. (5) we obtain

$$\left\langle \nabla T, \boldsymbol{s} \right\rangle = \left\langle \frac{\partial T}{\partial n}\boldsymbol{n} + \frac{\partial T}{\partial t_1}\boldsymbol{t}_1 + \frac{\partial T}{\partial t_2}\boldsymbol{t}_2, \boldsymbol{s} \right\rangle = \frac{\partial T}{\partial n}\left\langle \boldsymbol{n}, \boldsymbol{s} \right\rangle + \frac{\partial T}{\partial t_1}\left\langle \boldsymbol{t}_1, \boldsymbol{s} \right\rangle + \frac{\partial T}{\partial t_2}\left\langle \boldsymbol{t}_2, \boldsymbol{s} \right\rangle \tag{14}$$

and the BC given by Eq. (5) is transformed into the form

$$\frac{\partial T}{\partial n}\left\langle \boldsymbol{n}, \boldsymbol{s} \right\rangle + \frac{\partial T}{\partial t_1}\left\langle \boldsymbol{t}_1, \boldsymbol{s} \right\rangle + \frac{\partial T}{\partial t_2}\left\langle \boldsymbol{t}_2, \boldsymbol{s} \right\rangle = \delta g. \tag{15}$$

We define indices $i = 1, \ldots, n_1$, $j = 1, \ldots, n_2$ and $k = 1, \ldots, n_3$ in the direction of the height H, latitude B and longitude L, where n_1, n_2, n_3 denote the numbers of discretization intervals in height, meridional and zonal direction. Then we set approximations of normal and tangent vectors

$$\boldsymbol{n} = \left(\frac{x_{i-1,j,k} - x_{i,j,k}}{\left| \boldsymbol{x}_{i-1,j,k} - \boldsymbol{x}_{i,j,k} \right|}, \frac{y_{i-1,j,k} - y_{i,j,k}}{\left| \boldsymbol{x}_{i-1,j,k} - \boldsymbol{x}_{i,j,k} \right|}, \frac{z_{i-1,j,k} - z_{i,j,k}}{\left| \boldsymbol{x}_{i-1,j,k} - \boldsymbol{x}_{i,j,k} \right|} \right), \tag{16}$$

$$\boldsymbol{t}_1 = \left(\frac{x_{\mathrm{EN}} - x_{\mathrm{WS}}}{\left| \boldsymbol{x}_{\mathrm{EN}} - \boldsymbol{x}_{\mathrm{WS}} \right|}, \frac{y_{\mathrm{EN}} - y_{\mathrm{WS}}}{\left| \boldsymbol{x}_{\mathrm{EN}} - \boldsymbol{x}_{\mathrm{WS}} \right|}, \frac{z_{\mathrm{EN}} - z_{\mathrm{WS}}}{\left| \boldsymbol{x}_{\mathrm{EN}} - \boldsymbol{x}_{\mathrm{WS}} \right|} \right), \tag{17}$$

$$\boldsymbol{t}_2 = \left(\frac{x_{\mathrm{WN}} - x_{\mathrm{ES}}}{\left| \boldsymbol{x}_{\mathrm{WN}} - \boldsymbol{x}_{\mathrm{ES}} \right|}, \frac{y_{\mathrm{WN}} - y_{\mathrm{ES}}}{\left| \boldsymbol{x}_{\mathrm{WN}} - \boldsymbol{x}_{\mathrm{ES}} \right|}, \frac{z_{\mathrm{WN}} - z_{\mathrm{ES}}}{\left| \boldsymbol{x}_{\mathrm{WN}} - \boldsymbol{x}_{\mathrm{ES}} \right|} \right), \tag{18}$$

$\boldsymbol{x}_{i,j,k} = \left(x_{i,j,k}, y_{i,j,k}, z_{i,j,k} \right)$ is a representative point of the finite volume $p = (i, j, k)$, $\boldsymbol{x}_{\mathrm{WN}} = \left(x_{\mathrm{WN}}, y_{\mathrm{WN}}, z_{\mathrm{WN}} \right)$, $\boldsymbol{x}_{\mathrm{EN}} = \left(x_{\mathrm{EN}}, y_{\mathrm{EN}}, z_{\mathrm{EN}} \right)$, $\boldsymbol{x}_{\mathrm{WS}} = \left(x_{\mathrm{WS}}, y_{\mathrm{WS}}, z_{\mathrm{WS}} \right)$ and $\boldsymbol{x}_{\mathrm{ES}} = \left(x_{\mathrm{ES}}, y_{\mathrm{ES}}, z_{\mathrm{ES}} \right)$ are points in the corners of the bottom boundary Γ, and $\boldsymbol{x}_{i-(1/2),j,k} = \left(x_{i-(1/2),j,k}, y_{i-(1/2),j,k}, z_{i-(1/2),j,k} \right)$ is the point in the center of the bottom boundary Γ (see Fig. 2). In our numerical experiments, we consider the oblique vector in the form

$$\boldsymbol{s} = \left(\frac{x_{\mathrm{C}} - x_{i-(1/2),j,k}}{\left| \boldsymbol{x}_{\mathrm{C}} - \boldsymbol{x}_{i-(1/2),j,k} \right|}, \frac{y_{\mathrm{C}} - y_{i-(1/2),j,k}}{\left| \boldsymbol{x}_{\mathrm{C}} - \boldsymbol{x}_{i-(1/2),j,k} \right|}, \frac{z_{\mathrm{C}} - z_{i-(1/2),j,k}}{\left| \boldsymbol{x}_{\mathrm{C}} - \boldsymbol{x}_{i-(1/2),j,k} \right|} \right), \tag{19}$$

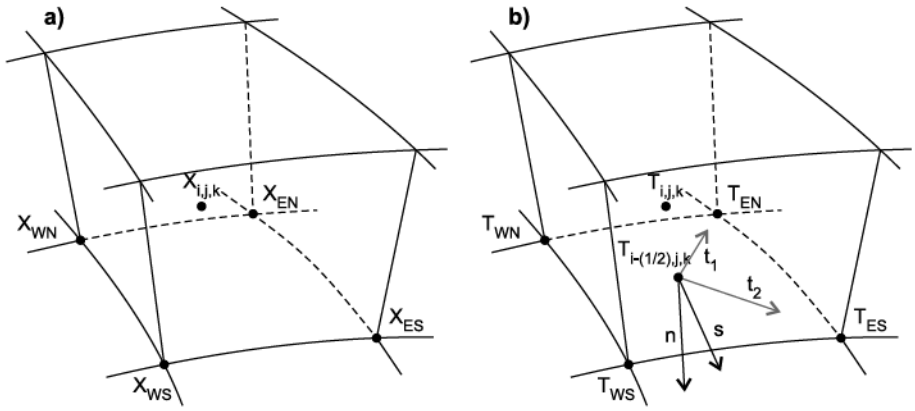

Fig. 2. Illustration of the computational grid for an approximation of the oblique derivative. **a)** $x_{i,j,k}$ denotes position vector of the center of volume and x_{WS}, x_{ES}, x_{EN}, x_{WN} are values of the position vectors of the vertices. **b)** $T_{i,j,k}$ denotes the value of the disturbing potential in the center of finite volume and T_{WS}, T_{ES}, T_{EN}, T_{WN} are values of the disturbing potential in the vertices. Vectors $\boldsymbol{t}_1$ and $\boldsymbol{t}_2$ denote independent tangent vectors to Γ and $\boldsymbol{n}$ the normal vector to Γ.

where $\boldsymbol{x}_C$ is the center point $\boldsymbol{x}_C = (x_C, y_C, z_C) \in R^3$ that is used to simulate the oblique vector in Section 4.1. In Sections 4.2 and 4.3, the real topography is used to calculate the oblique vector.

By $T_{i,j,k}$ we denote the approximate value of the solution T in the finite volume $p = (i, j, k)$ and we approximate the normal and tangential derivatives in Eq. (15) by

$$\frac{\partial T}{\partial n} = \frac{T_{i-1,j,k} - T_{i,j,k}}{\left| \boldsymbol{x}_{i-1,j,k} - \boldsymbol{x}_{i,j,k} \right|}, \tag{20}$$

$$\frac{\partial T}{\partial t_1} = \frac{T_{EN} - T_{WS}}{\left| \boldsymbol{x}_{EN} - \boldsymbol{x}_{WS} \right|}, \tag{21}$$

$$\frac{\partial T}{\partial t_2} = \frac{T_{WN} - T_{ES}}{\left| \boldsymbol{x}_{WN} - \boldsymbol{x}_{ES} \right|}, \tag{22}$$

where T_{WN}, T_{EN}, T_{WS}, T_{ES} (see Fig. 2) are defined by

$$\begin{aligned}
T_{WN} = \frac{1}{8}\big(& T_{i,j,k} + T_{i,j-1,k} + T_{i,j,k-1} + T_{i,j-1,k-1} \\
& + T_{i-1,j,k} + T_{i-1,j-1,k} + T_{i-1,j,k-1} + T_{i-1,j-1,k-1} \big), \\
T_{EN} = \frac{1}{8}\big(& T_{i,j,k} + T_{i,j-1,k} + T_{i,j,k+1} + T_{i,j-1,k+1} \\
& + T_{i-1,j,k} + T_{i-1,j-1,k} + T_{i-1,j,k+1} + T_{i-1,j-1,k+1} \big), \\
T_{WS} = \frac{1}{8}\big(& T_{i,j,k} + T_{i,j+1,k} + T_{i,j,k-1} + T_{i,j+1,k-1} \\
& + T_{i-1,j,k} + T_{i-1,j+1,k} + T_{i-1,j,k-1} + T_{i-1,j+1,k-1} \big), \\
T_{ES} = \frac{1}{8}\big(& T_{i,j,k} + T_{i,j+1,k} + T_{i,j,k+1} + T_{i,j+1,k+1} \\
& + T_{i-1,j,k} + T_{i-1,j+1,k} + T_{i-1,j,k+1} + T_{i-1,j+1,k+1} \big).
\end{aligned}$$

If we insert these approximations into Eq. (15) to get a discrete form of the oblique derivative BC given by Eq. (5)

$$\begin{aligned}
\langle \nabla T, \boldsymbol{s} \rangle \approx & \frac{T_{i-1,j,k} - T_{i,j,k}}{\left| \boldsymbol{x}_{i-1,j,k} - \boldsymbol{x}_{i,j,k} \right|} \langle \boldsymbol{n}, \boldsymbol{s} \rangle + \frac{T_{EN} - T_{WS}}{\left| \boldsymbol{x}_{EN} - \boldsymbol{x}_{WS} \right|} \langle \boldsymbol{t}_1, \boldsymbol{s} \rangle \\
& + \frac{T_{WN} - T_{ES}}{\left| \boldsymbol{x}_{WN} - \boldsymbol{x}_{ES} \right|} \langle \boldsymbol{t}_2, \boldsymbol{s} \rangle = \delta g .
\end{aligned} \tag{23}$$

These equations are incorporated into the FVM linear system of equations which is then solved.

4. NUMERICAL EXPERIMENTS

In this section, we present several numerical experiments where we have solved the problem given by Eqs (4)–(6) by the FVM. For numerical experiments a program in Mathematica 8.0 was created and then, in order to accelerate the computations, program in C programming language was developed.

4.1. Experimental order of convergence of the proposed approach

In the first numerical experiment, the computational domain has been a tesseroid bounded by two concentric spheres with radii $r_1 = 1$ and $r_2 = 2$, and by a coaxial cone with dimension $(0, \pi)\times(0, \pi)$. There have been the oblique derivative BC on the bottom and the Dirichlet BC on the upper and side boundaries applied. The center point has been shifted $x_C = (0.1, -0.2, -0.1)$. As the Dirichlet BC we have considered the exact solution of Eq. (4) in the form $T(x) = 1/r$, where r is the distance from x to the center point x_C. As the oblique derivative BC on the bottom boundary, we have prescribed the derivative of this exact solution which is equal to $-1/r^2$. The results can be seen in Table 1. One can observe that in the case when the center point is shifted, the proposed approach is second order accurate, i.e. the *EOC* (Experimental Order of Convergence) is more than 2.

For the second numerical experiment we have the same computational domain and the same BCs as in the previous experiment, but the oblique vector s has been rotated by 20°. The coordinates of the center point have been $x_C = (-0.2, 0.1, 0.2)$ and the Dirichlet and oblique derivative BC as well as the exact solution have been computed the same way as before. The $L_2(\Omega)$-norm of differences between the exact and numerical solutions are shown in Table 2. One can see that also in the case with the rotated oblique vector, the value of *EOC* is more than 2.

Table 1. The $L_2(\Omega)$-norm of differences between the exact and numerical solutions and the Experimental Order of Convergence (*EOC*) for the experiment with the shifted center point $x_C = (0.1, -0.2, -0.1)$. n_1, n_2 and n_3 denote numbers of discretization intervals in radial, meridional and zonal direction.

$n_1 \times n_2 \times n_3$	$\lvert T - T \rvert_{L_2(\Omega)}$	*EOC*
$2 \times 2 \times 4$	6.74805×10^{-2}	
$4 \times 4 \times 8$	9.00317×10^{-3}	2.90597
$8 \times 8 \times 16$	1.54266×10^{-3}	2.54502
$16 \times 16 \times 16$	3.01950×10^{-4}	2.35328
$32 \times 32 \times 64$	0.67123×10^{-5}	2.16928

Table 2. The same as in Table 1, but for the shifted center point $x_C = (-0.2, 0.1, 0.2)$ and the oblique vector s rotated by 20°.

$n_1 \times n_2 \times n_3$	$\|T - T\|_{L_2(\Omega)}$	*EOC*
$2 \times 2 \times 4$	6.43828×10^{-2}	
$4 \times 4 \times 8$	8.14779×10^{-3}	2.98220
$8 \times 8 \times 16$	1.34261×10^{-3}	2.60137
$16 \times 16 \times 16$	2.44307×10^{-4}	2.45827
$32 \times 32 \times 64$	0.52002×10^{-5}	2.23204

It is worth noting that in the case when the oblique vector is identical with a gradient vector, we can project to the normal without incorporating error. However, if this is not so (and this is the case of rotation), we can't solve the BVP with the Neumann BC and we have to use the BVP with the oblique derivative BC instead. The detailed study can be found in *Macák et al. (2012)*.

4.2. Numerical experiments using the EGM2008

This experiment has dealt with the fixed gravimetric BVP and the computational domain Ω above the Himalaya region approximated by the WGS84 reference ellipsoid. A range for the ellipsoidal latitude and longitude has been $B \in \langle 20.0°, 50.0° \rangle$ and $L \in \langle 60.0°, 110.0° \rangle$, respectively. To calculate the oblique derivative vector, the ellipsoidal heights above the WGS84 have been generated from SRTM30 (*Becker et al., 2009*). The upper boundary has been at the altitude of 240 km above the WGS84. The number of finite volumes has been 1200 in the height, 900 in the meridional and 1500 in the zonal directions, i.e. $200\ \mathrm{m} \times 2' \times 2'$ sized volumes have been created. All BCs, namely surface gravity disturbances as well as the disturbing potential, have been generated from EGM2008, see *Pavlis et al. (2008)*. The disturbing potential as a direct numerical solution to the BVP with the oblique derivative BC is depicted in Fig. 3. The differences between solution to the BVP with the oblique derivative BC and solution to the BVP with the Neumann BC can be seen in Fig. 4. One can observe that the highest values of differences are in the areas of the mountainous ridges. Statistics of differences between the solution to BVP with the oblique derivative BC and EGM2008 as well as differences between the BVP with the Neumann BC and EGM2008 is presented in Table 3. It is evident that solution to the BVP with the oblique derivative BC converges better to EGM2008 than the solution to the BVP with the Neumann BC.

4.3. Numerical experiments with real data

The first numerical experiment with real data has dealt with the same computational domain and the resolution as the numerical experiment in Subsection 4.2 only the BCs

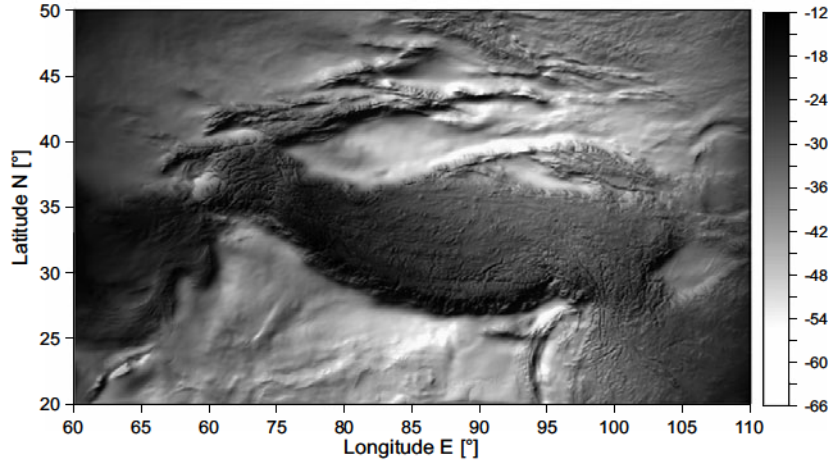

Fig. 3. The disturbing potential solution T of the boundary-value problem (Eq. (4), values in geopotential units, 1 GPU = 10 m^2 s^{-2}) with the oblique derivative boundary condition in area of Himalaya region using EGM2008 data only.

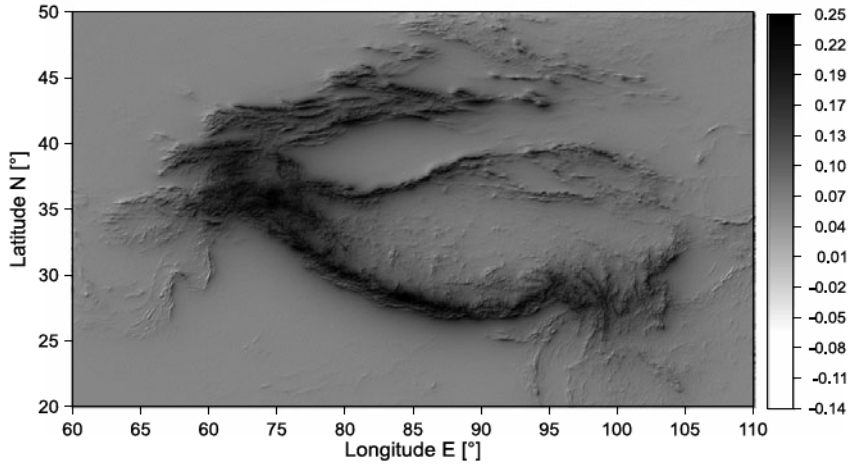

Fig. 4. Differences (values in GPU) between solution to the boundary-value problem with the oblique derivative boundary condition and solution to the boundary-value problem with the Neumann boundary condition when using EGM2008 data only.

have been changed. The input surface gravity disturbances have been transformed from the DTU10-GRAV gravity anomalies (*Andersen, 2010*) and the disturbing potential on side and upper boundary has been generated from the GOCO03S satellite only geopotential model up to degree 250 (*Mayer-Gürr et al., unpublished data*). We have

Table 3. Statistics of residuals (values in GPU) between the disturbing potential obtained by solving the boundary-value problem (BVP) with the oblique derivative boundary condition (BC) and the BVP with the Neumann BC, and the disturbing potential generated from EGM2008 directly. All BCs in BVPs have been generated from EGM2008. *RMS*: root mean square.

Residuals = T(BVP) – T(EGM2008)		
	BVP with the Neumann BC	BVP with the oblique derivative BC
Min	–0.227	–0.087
Mean	0.009	0.004
Max	0.332	0.095
St.Dev.	0.031	0.017
RMS	0.032	0.018

solved both BVPs, i.e. with the oblique derivative as well as with the Neumann BCs. The computation of each experiment took approximately 4.5 hours on 100 processors using 256 GB of RAM. The differences between both solutions are depicted in Fig. 5. One can see that the main differences are again in the zones with the mountainous ridges. Comparison of both solutions with EGM2008 is presented in Table 4. Again we have gained better statistical characteristics when taking the oblique derivative into account.

The second numerical experiment has dealt with the fixed gravimetric BVP in the domain Ω above Slovakia approximated by the WGS84 reference ellipsoid. The computational domain has been defined by the ellipsoidal latitude and longitude in range

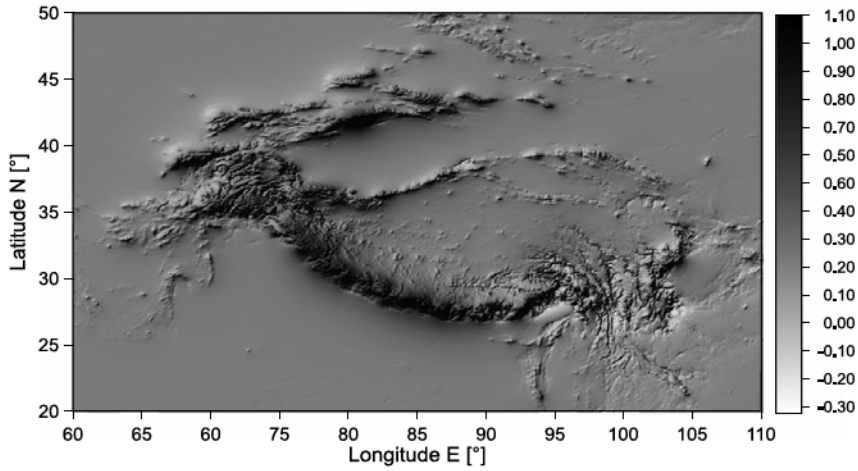

Fig. 5. Differences (values in GPU) between solutions to the boundary-value problem with the oblique derivative boundary condition and the boundary-value problem with the Neumann boundary condition when using real input data.

Table 4. Comparison of statistics (values in GPU) between the disturbing potential computed by the finite volume method applied to solving the boundary-value problem (BVP) with the Neumann boundary condition (BC) and the BVP with the oblique derivative BC, and the disturbing potential generated from EGM2008 directly. As input BCs, real data have been considered. *RMS*: root mean square.

Residuals = T(BVP) – T(EGM2008)		
	BVP with the Neumann BC	BVP with the oblique derivative BC
Min	–0.876	–0.438
Mean	–0.071	–0.025
Max	0.761	0.437
St.Dev.	0.075	0.042
RMS	0.104	0.049

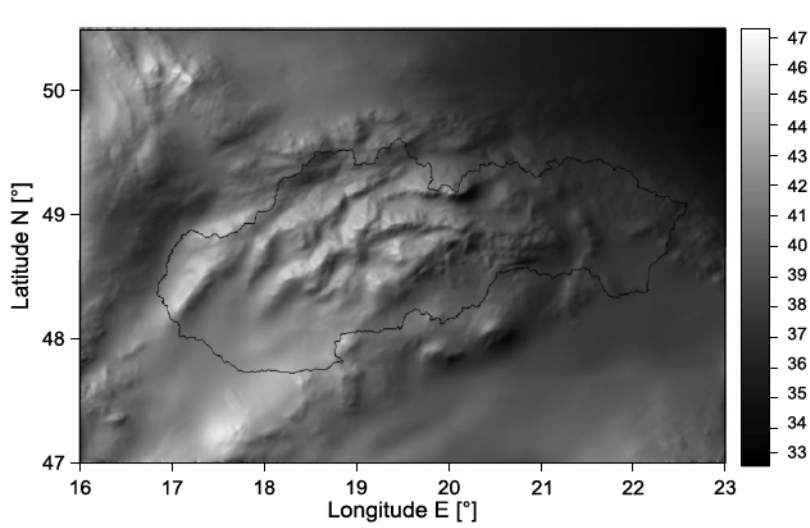

Fig. 6. The disturbing potential solution T (values in GPU) of the boundary-value problem with the oblique derivative boundary condition in Slovakia.

$B \in \langle 47.0^\circ, 55.5^\circ \rangle$ and $L \in \langle 16.0^\circ, 23.0^\circ \rangle$, respectively. Again, to calculate the oblique derivative vector, the ellipsoidal heights above the WGS84 have been generated from SRTM30 and the upper boundary has been at an altitude of 240 km. The number of discretization intervals has been 840 in height, 630 in meridional and 300 in zonal directions. As input data on the bottom boundary Γ, the surface gravity disturbances obtained from the original terrestrial gravimetric measurements have been considered. The disturbing potential on upper and side boundaries has been computed from the GOCO03S satellite only geopotential model up to degree 250. The FVM solution to the

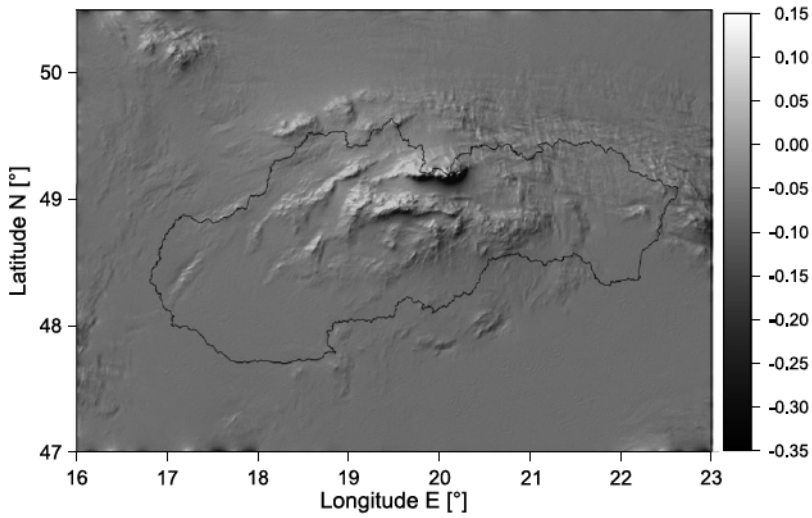

Fig. 7. The differences in quasigeoidal heights ζ (values in m) obtained as a solution to the boundary-value problem with the oblique derivative boundary condition and solution to the boundary-value problem with the Neumann boundary condition.

Table 5. The GPS/leveling test (values in m) at 61 points in area of Slovakia, where FEM denotes the solution presented in *Fašková et al. (2010)*, BEM the solution published in *Čunderlík et al. (2008)* and FFT (gravsoft) denotes the solution presented in *Mojzeš et al. (2005)*. All solutions are obtained without applying the fitting method. BC: boundary condition.

	Finite Volume Method		FEM	BEM	EGM2008	FFT (gravsoft)
	Neumann BC	Oblique BC				
Min	0.045	0.123	0.044	0.087	0.301	0.226
Mean	0.232	0.274	0.248	0.183	0.437	0.385
Max	0.393	0.419	0.394	0.624	0.584	0.523
St.Dev.	0.076	0.059	0.078	0.171	0.043	0.064

BVP with the oblique derivative BC is depicted in Fig. 6. The residuals between solutions to the BVP with Neumann BC and BVP with the oblique derivative BC can be seen in Fig. 7. The result of the GPS/leveling test at 61 points is presented in Table 5. The standard deviation of residuals at these GPS/levelling points in the case of the BVP with the Neumann BC is 7.6 cm, while in the case of the BVP with the oblique derivative BC is only 5.9 cm. Moreover, such standard deviation is lower than the standard deviation of solutions obtained by the approaches based on the boundary element method or the finite element method. It is worth noting that the treatment of incorporating the oblique derivative BC presented in this paper can be applied also in other numerical approaches.

5. CONCLUSIONS

We have presented the novel algorithm for solving the boundary-value problem with the oblique derivative boundary condition based on the decomposition of the oblique vector into one normal and two tangential components. As a numerical method has been implemented the finite volume method. The proposed numerical scheme has been tested by theoretical numerical experiments and we have obtained the second order accuracy of our approach. Then we have applied our algorithm to the fixed gravimetric boundary-value problem, namely, the numerical solution has been sought in the area of Himalaya region and in the area of Slovakia. In each experiment we have solved the boundary-value problem with the oblique derivative boundary condition and the boundary-value problem with the Neumann boundary condition. We have showed that with the same resolution and input data, we are able to obtain the more precise solution in areas with larger values of horizontal gradients when taking the oblique derivative boundary condition into account instead of the Neumann boundary condition. Moreover, the approach proposed in this paper can be easily implemented in other numerical approaches.

Acknowledgments: This work was supported by grant APVV-0072-11 and VEGA 1/1063/11. Calculations were performed in the Computing Center of the Slovak Academy of Sciences using the supercomputing infrastructure acquired in project ITMS 26240120025 (Slovak infrastructure for high-performance computing) supported by the Research and Development Operational Programme funded by the ERDF.

References

Andersen O.B., 2010. The DTU10 gravity field and mean sea surface. Second international symposium of the gravity field of the Earth (IGFS2), Fairbanks, Alaska (http://www.space.dtu.dk/english/~/media/Institutter/Space/English/scientific_data_and_models/global_marine_gravity_field/dtu10.ashx).

Becker J.J., Sandwell D.T., Smith W.H.F., Braud J., Binder B., Depner J., Fabre D., Factor J., Ingalls S., Kim S-H., Ladner R., Marks K., Nelson S., Pharaoh A., Trimmer R., Von Rosenberg J., Wallace G. and Weatherall P., 2009. Global bathymetry and elevation data at 30 arc seconds resolution: SRTM30 PLUS. *Mar. Geod.*, **32**, 355–371.

Bjerhammar A. and Svensson L., 1983. On the geodetic boundary value problem for a fixed boundary surface: A satellite approach. *Bull. Geod.*, **57**, 382–393.

Čunderlík R., Mikula K. and Mojzeš M., 2008. Numerical solution of the linearized fixed gravimetric boundary-value problem. *J. Geodesy*, **82**, 15–29.

Čunderlík R. and Mikula K., 2010. Direct BEM for high-resolution global gravity field modelling. *Stud. Geophys. Geod.*, **54**, 219–238.

Eymard R., Gallouët T. and Herbin R., 2001. Finite volume approximation of elliptic problems and convergence of an approximate gradient. *Appl. Numer. Math.*, **37**, 31–53.

Fašková Z., Čunderlík R. and Mikula K., 2010. Finite element method for solving geodetic boundary value problems. *J. Geodesy*, **84**, 135–144.

Holota P., 1997. Coerciveness of the linear gravimetric boundary-value problem and a geometrical interpretation. *J. Geodesy*, **71**, 640–651.

Holota P. and Nesvadba O., 2008. Model refinements and numerical solution of weakly formulated boundary-value problems in physical geodesy. In: Xu P., Liu J. and Dermanis A. (Eds), *VI Hotine-Marussi Symposium on Theoretical and Computational Geodesy*. International Association of Geodesy Symposia **132**. Springer-Verlag, Berlin, Germany, 320–326.

Klees R., 1995. Boundary value problems and approximation of integral equations by finite elements. *Manuscripta Geodaetica*, **20**, 345–361.

Klees R., van Gelderen M., Lage C. and Schwab C., 2001. Fast numerical solution of the linearized Molodensky problem. *J. Geodesy*, **75**, 349–362.

Koch K.R. and Pope A.J., 1972. Uniqueness and existence for the godetic boundary value problem using the known surface of the Earth. *Bull. Geod.*, **46**, 467–476.

Lehmann R., 1999. Boundary-value problems in the complex world of geodetic measurments. *J. Geodesy*, **73**, 491–500.

Lehmann R. and Klees R., 1999. Numerical solution of geodetic boundary value problems using a global reference field. *J. Geodesy*, **73**, 543–554.

Macák M., Mikula K. and Minarechová Z., 2012. Solving the oblique derivative boundaryvalue problem by the finite volume method. In: Handlovičová A., Minarechová Z. and Ševčovič D. (Eds), *ALGORITMY 2012. 19th Conference on Scientific Computing, Vysoké Tatry-Podbanské, Slovakia, September 9-14, 2012*. Slovak University of Technology in Bratislava, Bratislava, Slovakia, 75–84.

Mojzeš M., Janák J. and Papčo J., 2005. Gravimetric model of quasigeoid in the area of Slovakia. *Acta Montanistica Slovaca*, **10**, 161–165.

Pavlis N.K., Holmes S.A., Kenyon S.C. and Factor J.K., 2012. The development and evaluation of the Earth Gravitational Model 2008 (EGM2008). *J. Geophys. Res.*, **117**, B04406, DOI: 10.1029/2011JB008916.

Tscherning C.C., Knudsen P. and Forsberg R., 1994. *Description of the GRAVSOFT Package*. 4th Edition. Technical Report, Geophysical Institute, University ofCopenhagen, Copenhagen Denmark.